

MTG-FCI: ATBD for Active Fire Monitoring Product

Doc.No. : EUM/MTG/DOC/10/0613
Issue : v2
Date : 14 January 2013
WBS : MTG-834200

EUMETSAT
Eumetsat-Allee 1, D-64295 Darmstadt, Germany
Tel: +49 6151 807-7
Fax: +49 6151 807 555
<http://www.eumetsat.int>

Document Change Record

<i>Issue / Revision</i>	<i>Remarks</i>
v1 Draft	For internal review
v1B of 17 January 2011	First published version
v1C of 14 October 2011	Second published version following the recommendations of the System PDR Science Panel
v2 of 14 January 2013	Editorial changes in sections 3.3 and 3.5.1 after external review and after the internal review of the MTG-FCI PGS

Table of Contents

1	Introduction	4
1.1	Purpose of this Document	4
1.2	Structure of this Document	4
1.3	Applicable and Reference Documents	4
1.4	Acronyms and Definitions	5
2	Overview	7
2.1	Relevant Instrument Characteristics	7
2.2	Generated Products	9
3	Algorithm Description	10
3.1	Physical Basis Overview	10
3.2	Assumptions and Limitations	12
3.3	Algorithm Basis Overview	12
3.4	Algorithm Input	13
3.4.1	Primary Sensor Data	13
3.4.2	Ancillary Dynamic Data	14
3.4.3	Ancillary Static Data	15
3.5	Detailed Description	16
3.5.1	Description of the Threshold Tests	16
3.5.2	Derivation of the Thresholds	16
3.6	Output Description	20
4	Future Developments	21
5	Glossary of Terms Used in Equations	22

1 INTRODUCTION

1.1 Purpose of this Document

This document describes the algorithm theoretical basis for the Active Fire Monitoring (FIR) product, as it shall be derived from the Meteosat Third Generation Flexible Combined Imager (MTG-FCI).

1.2 Structure of this Document

Section 2 of this document provides a short overview over the MTG imaging instrument characteristics and the derived meteorological products, which will be referenced later in the text. This is followed by a detailed description of the underlying algorithm of the FIR product – its physical basis, the required input data, and a more detailed description of the product retrieval method. Section 4 describes possible future developments of the FIR algorithm.

A full list of acronyms is provided in section 1.4, literature references are listed in the following section. A glossary of the equation symbols used in this document can be found in section 5.

1.3 Applicable and Reference Documents

The following documents have been used to establish this document:

<i>Doc ID</i>	<i>Title</i>	<i>Reference</i>
[AD-1]	MTG End Users Requirements Document	EUM/MTG/SPE/07/0036
[AD-2]	MTG Products in the Level-2 Processing Facility	EUM/C/70/10/DOC/08
[AD-3]	MTG-FCI: ATBD for Radiative Transfer Model	EUM/MTG/DOC/10/0382
[AD-4]	MTG-FCI: ATBD for Cloud Mask and Cloud Analysis Product	EUM/MTG/DOC/10/0542
[AD-5]	MSG: Active Fire Monitoring with MSG - Algorithm Theoretical Basis Document	EUM/MET/REP/07/0170
[RD-1]	Amraoui, M., C.C. DaCamara, J.M.C. Pereira, 2010: Detection and monitoring of African vegetation fires using MSG-SEVIRI imagery	Remote Sens Environ., 114, 1038-1052. doi:10.1016/j.rse.2009.12.019.

Doc ID	Title	Reference
[RD-2]	Giglio L., J.D. Kendall, C.O. Justice, 1999: Evaluation of global fire detection algorithms using simulated AVHRR infrared data	Int. J. of Remote Sensing, Vol. 20, No. 10, pp. 1947-1985
[RD-3]	Giglio L., J. Descloitres, C.O. Justice, Y.J. Kaufman 2003: An Enhanced Contextual Fire Detection Algorithm for Modis.	Remote Sensing of Environment, Vol. 87, pp. 273-282
[RD-4]	Loveland T.R. and Belward A.S., 1997: The IGBP-DIS global 1km land cover data set, DISCover: first results.	Int. Journal of Remote Sensing, Vol. 18, No. 15, pp. 3289
[RD-5]	Morisette J.T., L. Giglio, I. Csizsar, C.O. Justice, 2005: Validation of the MODIS active fire product over Southern Africa with ASTER data.	Int. Journal of Remote Sensing, Vol. 26, No. 19, pp. 4239-4264
[RD-6]	Weaver J.F. and J.F. Purdom, 1995: Observing Forest Fires with the GOES-8, 3.9 μ m Imaging Channel.	Weather and Forecasting, Vol. 10, pp. 803-808

1.4 Acronyms and Definitions

The following table lists definitions for all acronyms used in this document.

Acronym	Full Name
AER	Aerosol Product
AMV	Atmospheric Motion Vectors
ASR	All Sky Radiance
ATBD	Algorithm Theoretical Basis Document
CMA	Cloud Mask
CRM	Clear Sky Reflectance Map
CT	Cloud Type
CTTH	Cloud Top Temperature and Height
FCI	Flexible Combined Imager
FCI-FDSS	FCI Full Disc Scanning Service
FCI-RSS	FCI Rapid Scanning Service
FDHSI	Full Disc High Spectral Resolution Imagery
GII	Global Instability Indices
HRFI	High Spatial Resolution Fast Imagery
HRV	High Resolution Visible Channel of SEVIRI
IR	Infrared
LUT	Lookup Table
MSG	Meteosat Second Generation
MTG	Meteosat Third Generation

Acronym	Full Name
NWP	Numerical Weather Prediction
OCA	Cloud Product (Optimal Cloud Analysis)
OLR	Outgoing Longwave Radiation
RTM	Radiative Transfer Model
RTTOV	Radiative Transfer for TOVS
SCE	Scene Identification
SAF	Satellite Application Facility
SEVIRI	Spinning Enhanced Visible and Infrared Imager
SSD	Spatial Sampling Distance
TIROS	Television and Infrared Observation Satellite
TOVS	TIROS Operational Vertical Sounder
TOZ	Total Column Ozone
VIS	Visible (solar)
VOL	Volcanic Ash Product

2 OVERVIEW

2.1 Relevant Instrument Characteristics

The mission of the Meteosat Third Generation (MTG) System is to provide continuous high spatial, spectral and temporal resolution observations and geophysical parameters of the Earth / Atmosphere System derived from direct measurements of its emitted and reflected radiation using satellite based sensors from the geo-stationary orbit to continue and enhance the services offered by the Second Generation of the Meteosat System (MSG) and its main instrument SEVIRI.

The meteorological products described in this document will be extracted from the data of the Flexible Combined Imager (FCI) mission. The FCI is able to scan either the full disc in 16 channels every 10 minutes with a spatial sampling distance in the range 1 – 2 km (Full Disc High Spectral Resolution Imagery (FDHSI) in support of the Full Disc Scanning Service (FCI-FDSS)) or a quarter of the earth in 4 channels every 2.5 minutes with doubled resolution (High spatial Resolution Fast Imagery (HRFI) in support of the Rapid Scanning Service (FCI-RSS)).

FDHSI and HRFI scanning can be interleaved on a single satellite (e.g. when only one imaging satellite is operational in orbit) or conducted in parallel when 2 satellites are available in orbit. Table 1 provides an overview over the FCI spectral channels and their respective spatial resolution.

The FCI acquires the spectral channels simultaneously by scanning a detector array per spectral channel in an east/west direction to form a swath. The swaths are collected moving from south to north to form an image per spectral channel covering either the full disc coverage or the local area coverage within the respective repeat cycle duration. Radiance samples are created from the detector elements at specific spatial sample locations and are then rectified to a reference grid, before dissemination to the End Users as Level 1 datasets. Spectral channels may be sampled at more than one spatial sampling distance or radiometric resolution, where the spectral channel has to fulfil FDHSI and HRFI missions or present data over an extended radiometric measurement range for fire detection applications.

Table 1: Channel specification for the Flexible Combined Imager (FCI)

<i>Spectral Channel</i>	<i>Central Wavelength, λ_0</i>	<i>Spectral Width, $\Delta\lambda_0$</i>	<i>Spatial Sampling Distance (SSD)</i>
VIS 0.4	0.444 μm	0.060 μm	1.0 km
VIS 0.5	0.510 μm	0.040 μm	1.0 km
VIS 0.6	0.640 μm	0.050 μm	1.0 km 0.5 km ^{#1}
VIS 0.8	0.865 μm	0.050 μm	1.0 km
VIS 0.9	0.914 μm	0.020 μm	1.0 km
NIR 1.3	1.380 μm	0.030 μm	1.0 km
NIR 1.6	1.610 μm	0.050 μm	1.0 km
NIR 2.2	2.250 μm	0.050 μm	1.0 km 0.5 km ^{#1}
IR 3.8 (TIR)	3.800 μm	0.400 μm	2.0 km 1.0 km ^{#1}
WV 6.3	6.300 μm	1.000 μm	2.0 km
WV 7.3	7.350 μm	0.500 μm	2.0 km
IR 8.7 (TIR)	8.700 μm	0.400 μm	2.0 km
IR 9.7 (O ₃)	9.660 μm	0.300 μm	2.0 km
IR 10.5 (TIR)	10.500 μm	0.700 μm	2.0 km 1.0 km ^{#1}
IR 12.3 (TIR)	12.300 μm	0.500 μm	2.0 km
IR 13.3 (CO ₂)	13.300 μm	0.600 μm	2.0 km

^{#1}: The spectral channels VIS 0.6, NIR 2.2, IR 3.8 and IR 10.5 are delivered in both FDHSI sampling and a HRFI sampling configurations.

2.2 Generated Products

The agreed list of MTG-FCI Level 2 products is detailed in [AD-2] and is repeated here for easy reference:

1. **SCE:**
Scene Identification (cloudy, cloud free, dust, volcanic ash, fire)
2. **OCA:**
Cloud Product (cloud top height and temperature, cloud top phase, cloud top effective particle size, cloud optical depth, cloud sub-pixel fraction)
3. **ASR:**
All Sky Radiance (mean IR radiance on a $n \times n$ pixel grid, together with other statistical information, for different scenes)
4. **CRM:**
Clear Sky Reflectance Map (VIS reflectance for all non-absorbing channels, accumulated over time)
5. **GII:**
Global Instability Indices (a number of atmospheric instability indices and layer precipitable water contents)
6. **TOZ:**
Total Column Ozone
7. **AER:**
Aerosol Product (asymmetry parameter, total column aerosol optical depth, refractive index, single scattering albedo, size distribution)
8. **AMV:**
Atmospheric Motion Vectors (vector describing the displacement of clouds or water vapour features over three consecutive images, together with a vector height)
9. **OLR:**
Outgoing Longwave Radiation (thermal radiation flux at the top of the atmosphere leaving the earth-atmosphere system)

The products will be derived from the spectral channel information provided by the FDHSI mission, on the resolution detailed in [AD-2].

An important tool for product extraction is a radiative transfer model (RTM), as described in [AD-3]. The IR model choice for the Level 2 product extraction is RTTOV, which is developed and maintained by the Satellite Application Facility on Numerical Weather Prediction (NWP-SAF). An RTM for solar channels is likely to be product specific and is yet to be fully determined.

This ATBD describes the algorithm of the active fire monitoring product (FIR). The product will be derived over a certain processing area, defined as pixels lying within a great circle arc of pre-defined size around the subsatellite point (typically 70°).

3 ALGORITHM DESCRIPTION

3.1 Physical Basis Overview

The active fire monitoring product (FIR) derived from geostationary imager data is an important product to serve the environmental protection community.

Forest and vegetation fires have typical temperatures in the range of 500 K to 1000 K. According to Planck's law

$$B(\lambda, T) = \frac{2hc^2}{\lambda^5} \frac{1}{e^{\frac{hc}{\lambda kT}} - 1} \quad (1)$$

$B(\lambda, T)$: spectral radiance per unit solid angle for wavelength λ and temperature T
 h : Planck constant
 c : speed of light
 k : Boltzmann constant

the peak emission of radiance for blackbody surfaces of such temperatures is between 3 and 5.8 μm (thus best observed by MTG-FCI channel IR 3.8). For an ambient temperature of 290 K, the peak of radiance emission is located at approximately 10 μm (corresponding to MTG-FCI channel IR 10.5). Figure 1 illustrates this concept.

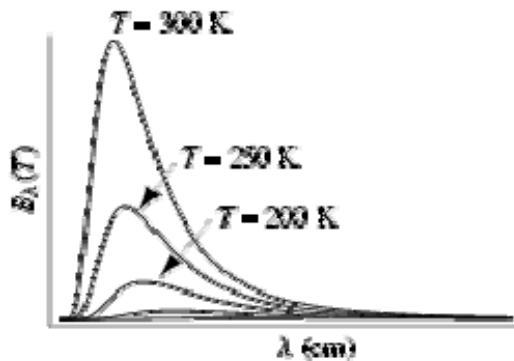


Figure 1: Graphical illustration of Planck's law for three different temperatures

This shift of peak emission goes together with a higher relative sensitivity to temperature changes towards smaller wavelengths. This is important, as typical wildfires are usually small "hot spots", much smaller than an MTG-FCI IR pixel. Such small fires have an only negligible effect on the IR 10.5 radiance, but a large effect in channel IR 3.8. The following example illustrates this:

A temperature difference of the emitting surface of only 5 K at 300 K increases the radiance at 11 μm wavelength by $\sim 7\%$.

The same temperature difference, however, increases the radiance at 4 μm wavelength by $\sim 18\%$.

Active fire detection algorithms from remote sensing use this shift of the peak emission and the increases sensitivity to temperature changes to detect such hot spots within a given pixel, which are usually fires of sub-pixel size. The sensitivity of the channel IR 3.8 to hot spots is so high that it shows small sub-pixel fires, which do not have any significant impact upon the IR 10.5 brightness temperature. Figure 2 shows a typical example of the respective MSG channels (IR 3.9 and IR 10.8).

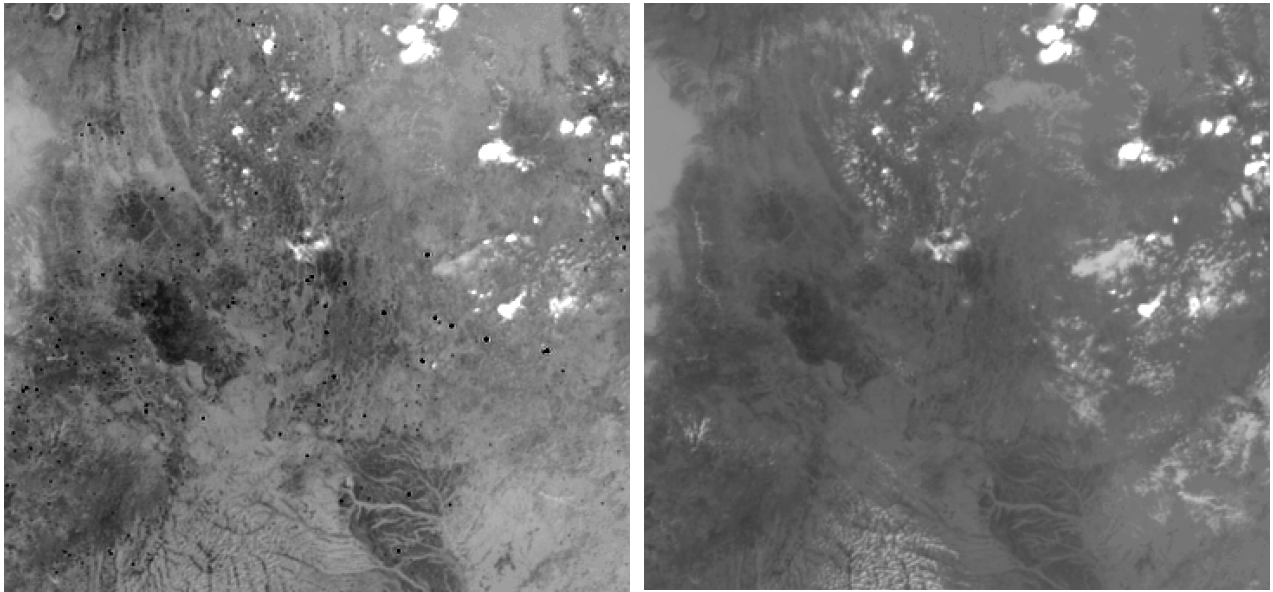


Figure 2: MSG examples of the IR 3.9 channel (left) and the IR 10.8 channel (right) for the same scene (29 July 2010, 1400 UTC over Central Africa). Wild fires are clearly visible in the IR 3.9 image as black hot spots.

However, the measurements in channel IR 3.8 are influenced by water vapour absorption, solar reflectance during day, and sub-pixel size clouds over hot surfaces.

The active fire detection algorithm aims at filtering out the active fires by a combination of threshold tests using channels IR 3.8 and IR 10.5. Both channels can be operated on a 2 km and a 1 km resolution, thus the algorithm needs to be in principle flexible to work on both resolutions.

The basic principles of the FIR algorithm are similar to those already in use for other instruments like GOES [RD-6], AVHRR [RD-2], and MODIS [RD-3], and MSG [AD-5] and [RD-6].

The FIR algorithm shall only be applied to land surfaces, which means that off-shore oil burning fires or fires on small islands (e.g. active volcanoes which also fall under the hot spot category) are not monitored by the algorithm. Bare soil land surfaces are also excluded from the processing. Pixels are considered as bare soil, if the surface types are desert or open shrub land, where this classification is taken from climatological background information for the MTG-FCI field of view. In addition, the IR 10.5-IR 8.7 difference is used to check for bare soil: Because of a smaller IR 8.7 surface emissivity for bare soil compared to the IR10.5 emissivity, the difference of the two channels is high in these cases. It should be noted that the active fire detection algorithm does not depend on the cloud mask, as the algorithm is

trying to filter out hot spots, which are in general much warmer than clouds. This concept also allows detecting fires under semi-transparent clouds.

3.2 Assumptions and Limitations

The current fire monitoring algorithm is able to detect most of the existing active fires with a minimum of false alarms.

The following conditions, however, can still lead to falsely detected fires:

- Mixed water (river/lake/coast) and land scenes under sun glint conditions
- Unknown land surface emissivity, in particular over inhomogeneous terrain with spatially variant emissivity
- Dusk and dawn periods with rapidly changing IR 3.8 values (see section 3.5.2, thresholds for fire classification depend on day or night conditions and are ill-defined during dusk and dawn).

Very small fires remain undetected due to the MTG-FCI radiometric performance. Examples of the general limitations for fire monitoring algorithms are given by [RD-5]

3.3 Algorithm Basis Overview

For the processed pixels, the FIR algorithm uses the following five criteria to check for potential fire and fire pixels:

- (1) Brightness temperature of channel IR 3.8 has to exceed a certain threshold
- (2) Brightness temperature difference of channels IR 3.8 and IR 10.5 has to exceed a certain threshold
- (3) Difference of the standard deviations of channel IR 3.8 and IR 10.5 has to exceed a certain threshold
- (4) Standard deviation of channel IR 10.5 has to be below a certain threshold
- (5) Standard deviation of channel IR 3.8 has to exceed a certain threshold

(all standard deviations are computed over a 3x3 pixel group, centred on the processing pixel)

Test (1):

This test identifies pixels with much warmer than expected IR 3.8 temperatures. Section 3.5.2 will explain how the "expected IR 3.8 temperatures are derived.

Test (2):

As channel IR 10.5 is much less sensitive to hot spots, the brightness temperature of IR 10.5 will not be as high as the brightness temperature in channel IR 3.8. This means that the brightness temperature difference of channels IR 3.8 and IR 10.5 is also higher than for non-fire pixels.

Test (3):

The difference of the standard deviation of channel IR 3.8 and the standard deviation of channel IR 10.5 over 3 x 3 pixels around a central hot spot is used to identify the real hot spot versus the natural (heated) background temperature of the surface. For active fires it is expected that the standard deviation for channel IR 3.8 is much larger than for channel IR 10.5. For other clear surfaces the standard deviation in both channels are approximately the same, while for clouds and cloud edges the standard deviation for channel IR 10.5 is larger than for channel IR 3.8.

Test (4):

The reduced sub-pixel fire sensitivity of IR 10.5 is used to correct for mis-classified fire pixels. Pixels that have passed the first three of the above tests can also be missed clouds, highly variable surface types or highly variable terrain elevation. The correction is done by using the standard deviation of channel IR 10.5, which will be relatively low in fire regions because the fire pixels have similar brightness temperatures as the surrounding non-fire areas.

Test (5):

The standard deviation of channel IR 3.8 over 3 x 3 pixels around a central hot spot is used to identify the real hot spot versus the natural (heated) background temperature of the surface. This test will, however, also pick up naturally hot surface spots and/or e.g. cloud edges.

The standard deviation is calculated on a 3x3 pixel array around each MTG-FCI pixel.

3.4 Algorithm Input

Table 2 lists the data that needs to be available at the start of the FIR processing.

3.4.1 Primary Sensor Data

For each pixel within the processing area, the brightness temperatures for the three IR MTG-FCI channels and the VIS 0.6 channel, as listed in Table 2, must be available.

The pixel resolution of the channel with the lowest resolution (i.e. IR 8.7, 2 km resolution) determines the resolution of the product. This means that the VIS 0.6 channel (1 km resolution) needs to be averaged to the coarser resolution.

Table 2: Necessary input data for the FIR processing

Parameter Description	Variable Name
Reflectances for MTG-FCI channel VIS0.6 for each pixel within the processing area	ρ
Brightness Temperatures for channels IR 3.8, IR 8.7, IR 10.5, for each pixel within the processing area	$T_B(\text{ch})^1$
Solar zenith and satellite zenith angles for each pixel within the processing area	$\zeta_{\text{sun}}, \zeta_{\text{sat}}$
Surface emissivity information, for the same three channels, for each pixel over the processing area	$\epsilon(\text{ch})$
Sun glint angle	ζ_{glint}
Radiances derived with RTTOV from ECMWF forecasts, interpolated to the image processing time. Needed RTTOV parameters: - Top of atmosphere clear sky radiance - Total transmittance - Downward radiance at surface level for channels IR3.8 and IR10.5	$r_{\text{top}}(\text{ch})$ $\tau_a(\text{ch})$ $r_{\text{down}}(\text{ch})$
Surface type information for each MTG-FCI pixel (land type, or sea)	$S\text{Type}_{\text{MTG}}$
Surface type information for the ECMWF grid points within the processing area (land or sea)	$S\text{Type}_{\text{ECMWF}}$
Distance to the nearest coast/lake shoreline (in pixel)	$N\text{Coast}_{\text{MTG}}$

¹: index (ch) refers to channels IR 3.8, IR 10.5

3.4.2 Ancillary Dynamic Data

The FIR product needs the RTTOV output, as stated in Table 2, interpolated to the pixel position from the adjacent RTTOV grid points:

For RTTOV-9, these are the parameters:

- $r_{\text{top}}(\text{ch})$ *radiance % clear* (for all relevant channels, in the "radiance type" RTTOV output)
- $\tau_a(\text{ch})$ *transmission % tau_total* (for all relevant channels, in the "transmission type" RTTOV output)
- $r_{\text{down}}(\text{ch})$ *radiance % dnclear* (for all relevant channels, at the lowest atmospheric level, in the "radiance type" RTTOV output)

As RTTOV provides the results on the ECMWF grid (which typically has a fixed latitude and longitude spacing), the results need to be interpolated to the pixel position:

Within the spatial interpolation of the ECMWF profiles, care has to be given to the actual surface type value of the forecast points compared to the (predominant) surface type of the FoR. Only such ECMWF grid points shall be used for the spatial interpolation, which have the same surface type (only land/sea are discriminated as two possible types).

If, for example, a specific FoR has surface type “land”, but a number of the surrounding ECMWF grid points have surface type “sea” (or vice versa), these grid points shall be disregarded in the spatial interpolation. Otherwise, coastal features will wrongly show up in the final product. Figure 3 shows a schematic of this process.

In case, however, that all surrounding ECMWF grid points differ in their surface type from the pixel's surface type (e.g. small islands or small lakes or rivers), all four surrounding grid points have to be used.

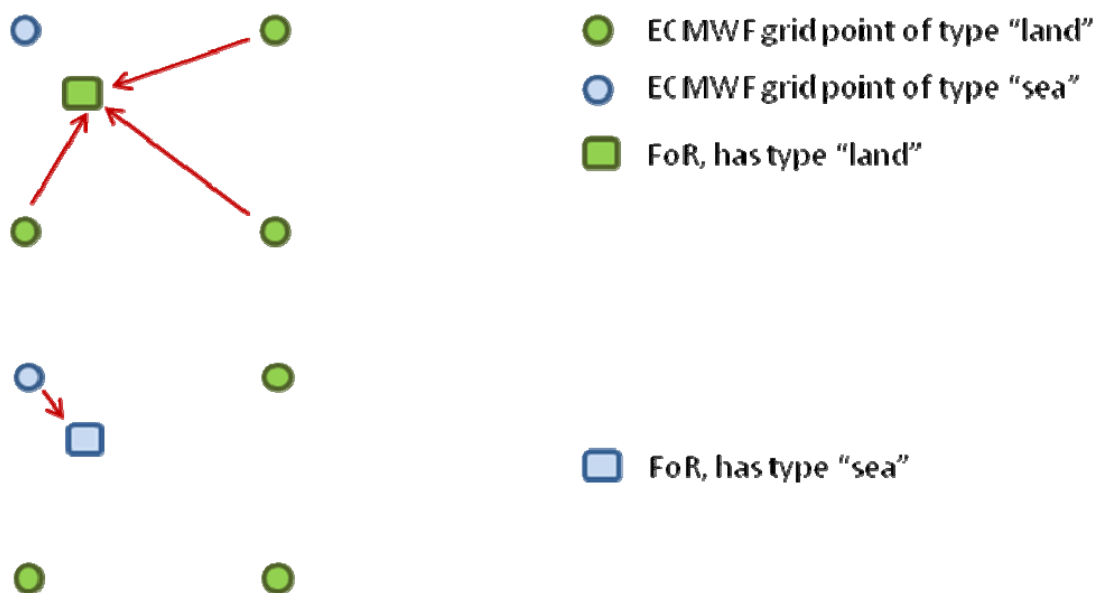


Figure 3: Schematic illustration of the use of forecast data depending on the FoR and the forecast grid surface type. Only the forecast data of the same surface type shall be used, as illustrated for the “land” case (top) and the “sea” case (bottom). The arrows denote which ECMWF grid points shall be used in these cases.

3.4.3 Ancillary Static Data

FIR uses the following ancillary static datasets:

- Pixel-based land-sea-mask/surface-type-map
- Pixel-based emissivity maps for the three infrared channels IR 3.8 and IR 10.5

The pixel-based land-sea-mask/surface-type-map consists of 17 different land surface types and one ocean/open water surface type. This map can be e.g. derived from the International Geosphere-Biosphere Programme (IGBP) surface type map [RD-4].

The pixel-based emissivity data is expected to be constant over a certain period (typically a month), so the processing has to allow for a possible time dependence in this input dataset.

3.5 Detailed Description

The algorithm distinguishes between "potential fires" and "fires": Pixels with a lower confidence as a result of the FIR processing are defined as "potential fire", those with a higher confidence are defined as "fire" (see section 3.5.1). The algorithm itself is based on a simple threshold algorithm. The FIR algorithm will be applied if the following conditions are all met:

- Pixel is land
- Pixel is not bare soil:
This information is taken from the pixel based surface type mask $S_{Type_{MTG}}$; in addition the brightness temperature difference $IR\ 8.7 - IR\ 10.5$ needs to be smaller than 4 K
- Pixel is at least 1 pixel length away from the nearest coastline (which can also be a river or lake coast), described by parameter $N_{Coast_{MTG}}$
- During day the reflectance ρ in channel VIS 0.6 is smaller than 15% (to exclude bare soil and small clouds)
- The sun glint angle ζ_{glint} is larger than 3° .

3.5.1 Description of the Threshold Tests

A pixel is classified as containing a "potential fire" if the following conditions are all met:

$T_B(IR\ 3.8)$	> threshold 1	(Test 1a)
$\sigma(T_B(IR\ 3.8)) - \sigma(T_B(IR\ 10.5))$	> threshold 2	(Test 2a)
$T_B(IR\ 3.8) - T_B(IR\ 10.5)$	> threshold 3	(Test 3a)
$\sigma(T_B(IR\ 10.5))$	< threshold 4	(Test 4)
$\sigma(T_B(IR\ 3.8))$	> threshold 5	(Test 5a)

A pixel is classified as containing a "fire" if in addition the following (stricter) conditions are all met:

$T_B(IR\ 3.8)$	> threshold 6	(Test 1b)
$\sigma(T_B(IR\ 3.8)) - \sigma(T_B(IR\ 10.5))$	> threshold 7	(Test 2b)
$T_B(IR\ 3.8) - T_B(IR\ 10.5)$	> threshold 8	(Test 3b)
$\sigma(T_B(IR\ 3.8))$	> threshold 9	(Test 5b)

T_B refers to brightness temperatures in the indicated channels, σ the respective standard deviation for the indicated brightness temperatures, computed over 3×3 pixels centred on the processing pixel. The nine different thresholds (threshold 1-9) are described in the next section.

3.5.2 Derivation of the Thresholds

As the brightness temperatures in the infrared channels change in the course of a day, and as the IR 3.8 channel has a solar contribution, which also changes during the day, the thresholds

1-9 as mentioned in section 3.5.1 are not fixed values, but are also defined such that they model the diurnal temperature cycle, i.e. the thresholds are dynamic.

In order to derive these dynamic thresholds, the algorithm uses the RTTOV results. As RTTOV uses unit emissivity values for all grid-points, the given top of the atmosphere clear sky radiance has to be corrected for the given (pixel-based) land surface emissivity. The emissivity corrected radiances for channels IR 3.8 and IR 10.5 consist of

- (a) The emission of the surface, multiplied by the atmospheric transmission of the entire atmosphere:

$$\varepsilon(\text{ch}) B_{\text{ch}}(T_{\text{skin}}) T_{\text{a}}(\text{ch})$$

$\varepsilon(\text{ch})$: emissivity for channel ch
 $B_{\text{ch}}(T_{\text{skin}})$: the spectral blackbody radiance for channel c for the surface skin temperature T_{skin}
 $T_{\text{a}}(\text{ch})$ total atmospheric transmittance for channel ch

- (b) Downwelling radiation reflected by the surface

$$(1 - \varepsilon(\text{ch})) L_{\text{down}}(\text{ch}) T_{\text{a}}(\text{ch})$$

$(1 - \varepsilon(\text{ch}))$: surface reflectivity for channel ch
 $L_{\text{down}}(\text{ch})$: downwelling radiance at surface level, for channel ch
 $T_{\text{a}}(\text{ch})$: total atmospheric transmittance for channel ch (as above)

- (c) Contribution from the atmosphere above the surface, which can be inferred from

$$L_{\text{top}}(\text{ch}) - B_{\text{ch}}(T_{\text{skin}}) T_{\text{a}}(\text{ch})$$

$L_{\text{top}}(\text{ch})$: total outgoing radiance at the top of the atmosphere for channel ch
 $B_{\text{ch}}(T_{\text{skin}})$: spectral blackbody radiance for channel ch for the surface skin temperature T_{skin} , as above
 $T_{\text{a}}(\text{ch})$ total atmospheric transmittance for channel ch, as above

- (d) In addition, for channel IR 3.8, its solar component needs to be considered according to

$$(1 - \varepsilon(\text{IR 3.8})) L_{\text{sol}}(\text{IR 3.8}) \cos(\zeta_{\text{sun}}) T_{\text{a}}(\text{IR 3.8})$$

during daylight hours, while the solar contribution is of course 0 at night.

$[1 - \varepsilon(\text{IR 3.8})]$: surface reflectivity in channel IR 3.8
 $L_{\text{sol}}(\text{IR 3.8})$: solar radiance at the top of the atmosphere, convolved with the IR 3.8 spectral response
 ζ_{sun} : local solar zenith angle
 $T_{\text{a}}(\text{IR 3.8})$: total atmospheric transmittance for channel IR 3.8

In summary, the IR 10.5 top of atmosphere radiance, corrected for the local surface emissivity, is

$$\begin{aligned}
 L_{\text{toa}}(\text{IR } 10.5) &= \varepsilon(\text{IR } 10.5) B_{\text{IR } 10.5}(T_{\text{skin}}) T_a(\text{IR } 10.5) + \\
 &\quad (1 - \varepsilon(\text{IR } 10.5)) L_{\text{down}}(\text{IR } 10.5) T_a(\text{IR } 10.5) + \\
 &\quad L_{\text{top}}(\text{IR } 10.5) - B_{\text{IR } 10.5}(T_{\text{skin}}) T_a(\text{IR } 10.5)
 \end{aligned} \tag{2}$$

and for channel IR 3.8, the corrected radiance is

$$\begin{aligned}
 L_{\text{toa}}(\text{IR } 3.8) &= \varepsilon(\text{IR } 3.8) B_{\text{IR } 3.8}(T_{\text{skin}}) T_a(\text{IR } 3.8) + (1 - \varepsilon(\text{IR } 3.8)) L_{\text{down}}(\text{IR } 3.8) T_a(\text{IR } 3.8) + \\
 &\quad L_{\text{top}}(\text{IR } 3.8) - B_{\text{IR } 3.8}(T_{\text{skin}}) T_a(\text{IR } 3.8) + \\
 &\quad (1 - \varepsilon(\text{IR } 3.8)) L_{\text{sol}}(\text{IR } 3.8) \cos(\zeta_{\text{sun}}) T_a(\text{IR } 3.8) T_a(\text{IR } 3.8)
 \end{aligned} \tag{3}$$

The following parameters are available from the RTTOV output (interpolated in time and to the respective pixel position), reference is RTTOV version 9:

transmission % tau_total(ch)	representing T_a (ch)
radiance % clear(ch)	representing $L_{\text{top}}(\text{ch})$ for $\varepsilon = 1$
radiance % dnclear(ch)	representing $L_{\text{down}}(\text{ch})$

$L_{\text{sol}}(\text{IR } 3.8)$ must be pre-computed from the solar spectrum and the IR 3.8 spectral response function (and should be weighted with the actual earth-sun distance).

The respective emissivities, the solar zenith angle and the surface skin temperature must be valid for the processed pixel for the corresponding acquisition time. These final radiances are then converted to brightness temperatures (for details on the radiance to brightness temperature conversion, see [AD-3], section 3.2), providing the "expected" or "predicted" brightness temperatures for the processed pixel, $T_{\text{B,pred}}(\text{IR } 3.8)$ and $T_{\text{B,pred}}(\text{IR } 10.5)$. The final thresholds depend on these predicted temperatures according to:

threshold 1	=	$T_{\text{B,pred}}(\text{IR } 3.8) + a_1 + a_2 \sin(\zeta_{\text{sat}})$
threshold 2	=	$a_3 + a_5 (\zeta_{\text{sat}} - a_4)$ if $a_3 + a_5 (\zeta_{\text{sat}} - a_4) < a_3$
threshold 2	=	a_3 if $a_3 + a_5 (\zeta_{\text{sat}} - a_4) \geq a_3$
threshold 3	=	$T_{\text{B,pred}}(\text{IR } 3.8) - T_{\text{B,pred}}(\text{IR } 10.5) + a_6 + a_7 \sin(\zeta_{\text{sat}})$
threshold 4	=	a_8
threshold 5	=	$a_9 + a_{11} (\zeta_{\text{sat}} - a_{10})$ if $a_9 + a_{11} (\zeta_{\text{sat}} - a_{10}) < a_9$
threshold 5	=	a_9 if $a_9 + a_{11} (\zeta_{\text{sat}} - a_{10}) \geq a_9$
threshold 6	=	$T_{\text{B,pred}}(\text{IR } 3.8) + b_1 + b_2 \sin(\zeta_{\text{sat}})$
threshold 7	=	$b_3 + b_5 (\zeta_{\text{sat}} - b_4)$ if $b_3 + b_5 (\zeta_{\text{sat}} - b_4) < b_3$
threshold 7	=	b_3 if $b_3 + b_5 (\zeta_{\text{sat}} - b_4) \geq b_3$
threshold 8	=	$T_{\text{B,pred}}(\text{IR } 3.8) - T_{\text{B,pred}}(\text{IR } 10.5) + b_6 + b_7 \sin(\zeta_{\text{sat}})$
threshold 9	=	$b_9 + b_{11} (\zeta_{\text{sat}} - b_{10})$ if $b_9 + b_{11} (\zeta_{\text{sat}} - b_{10}) < b_9$

$$\text{threshold 9} = b_9 \quad \text{if } b_9 + b_{11} (\zeta_{\text{sat}} - b_{10}) \geq b_9$$

It should be noted that this approach is only valid for satellite zenith angles ζ_{sat} up to 70° .

The coefficients a_1 to a_{11} and b_1 to b_{11} are highly empirical: Values for MSG-SEVIRI exist, which will need fine tuning for MTG-FCI. In addition, the coefficients are different for "day" and "night". In this context, "day" is defined for cases where

$$\zeta_{\text{sun}} < \zeta_{\text{sun,thresh}}$$

where $\zeta_{\text{sun,thresh}}$ is a certain cut-off solar zenith angle (e.g. 85°). "night" is defined for cases where

$$\zeta_{\text{sun}} > 90^\circ$$

For cases where

$$\zeta_{\text{sun,thresh}} \leq \zeta_{\text{sun}} \leq 90^\circ$$

the values of the coefficients need to be linearly interpolated between their respective day and night value. Although an MSG version of the coefficients a_1 to a_{11} and b_1 to b_{11} exists for MSG, (see Table 3), the values will need to be fine-tuned to account for possible spectral differences between MSG and MTG-FCI. This can be done during the commissioning phase of MTG-FCI.

Table 3: Coefficients a_1 to a_{11} and b_1 to b_{11} for MSG

Coeff	Day	Night
a_1	5	0
a_2	5	5
a_3	2	2
a_4	60	60
a_5	0.25	0.25
a_6	0	0
a_7	0	0
a_8	4	4
a_9	1	1
a_{10}	60	60
a_{11}	0.25	0.25
b_1	10	5
b_2	5	5
b_3	4	4
b_4	60	60
b_5	0.25	0.25
b_6	0	0
b_7	0	0
b_8	0	0
b_9	1	1
b_{10}	60	60
b_{11}	0.25	0.25

Note: some coefficients are set to zero, thus in the MSG version having no effect, but might be useful after further tuning

3.6 Output Description

For each pixel the FIR output will contain the information whether the pixel has no fire, a potential fire or a fire.

4 FUTURE DEVELOPMENTS

The above description assumes an overall pixel resolution of 2 km for the channels VIS 0.6, IR 3.8, IR 8.7 and IR 10.5. As VIS 0.6, IR 3.8 and IR 10.5 will be all available on a 1 km resolution, the algorithm can in principle also be applied to this resolution: This will have the advantage of detecting more (smaller) fires. The only difference to the 2 km version is the use of the IR 8.7 channel: As outlined in section 3.5, this channel is only used to detect bare soil (through the brightness temperature difference IR 10.5 and IR 8.7) – this bare soil check can, however, also be done through the detailed surface type map and (during daytime) through the use of the VIS 0.6 channel.

Furthermore, section 3.5. states that the algorithm should be run over land pixels only: In principle, the algorithm will also work over sea areas, so a full disk application may be considered for MTG-FCI.

During the commissioning phase of MTG-FCI, the coefficients a_1 to a_{11} and b_1 to b_{11} need to be fine-tuned to account for possible spectral differences between MSG and MTG-FCI. In addition the thresholds (1-9) need to be fine-tuned during the commissioning phase of MTG-FCI.

Additional tests to filter out false alarms (e.g. standard deviation of the difference (IR3.8-IR10.5)) may also be tested.

5 GLOSSARY OF TERMS USED IN EQUATIONS

Variable Name	Meaning	Unit
$a_1 - a_{11}$	threshold coefficients	{various}
$b_1 - b_{11}$	threshold coefficients	{various}
B	Blackbody radiance according to Planck's Law	$\text{mW/m}^2/\text{ster/cm}^{-1}$
c	Speed of light	m/s
ch	channel index (here: IR 3.8 and IR 10.5)	n/a
h	Planck constant	J s
k	Boltzmann constant	J/K
$\text{NCoast}_{\text{MTG}}$	Distance to nearest coast line (for each pixel)	pixel
L_{down}	Downwelling radiance at surface level	$\text{mW/m}^2/\text{ster/cm}^{-1}$
L_{sol}	Solar radiance at the top of the atmosphere (IR 3.8)	$\text{mW/m}^2/\text{ster/cm}^{-1}$
L_{toa}	Radiance at top of atmosphere (for correct ϵ)	$\text{mW/m}^2/\text{ster/cm}^{-1}$
L_{top}	Radiance at top of atmosphere (for $\epsilon=1$ surface)	$\text{mW/m}^2/\text{ster/cm}^{-1}$
$\text{SType}_{\text{MTG}}$	Pixel based surface type	n/a
$\text{SType}_{\text{ECMWF}}$	Surface type of ECMWF grid points	n/a
T	Temperature	K
T_B	Brightness temperature	K
T_{skin}	Surface skin temperature	K
ϵ	Emissivity	n/a
λ	Wavelength	μm
ρ	Reflectance in channel VIS 0.6	%
σ	Brightness temperature standard deviation	K
T_a	atmospheric transmittance	n/a
ζ_{glint}	Sun glint angle	deg
ζ_{sat}	Satellite zenith angle	deg
ζ_{sun}	Solar zenith angle	deg
$\zeta_{\text{sun,thresh}}$	Threshold solar zenith angle to define "night" conditions	Deg